GPU-Accelerated Optical Simulation of Cherenkov Emission Under Different Beam Conditions

2026 JULY 19–22 VANCOUVER, BC
JOINT AAPM | COMP MEETING

Yifeng Zhu[1]; Baozhu Lu, PhD[1] and Timothy C. Zhu, PhD[1]
[1]Department of Radiation Oncology, School of Medicine, University of Pennsylvania, Philadelphia, PA 19104

ABSTRACT

Cherenkov imaging can provide real-time surface-dose information, but the detected signal varies with tissue optical properties and beam conditions. An in-house CUDA-based Monte Carlo framework was developed to simulate wavelength-dependent Cherenkov photon generation and transport. The code was validated using nine silicone phantoms and a simplified normally incident electron source distributed from 0–1 cm beneath the surface. For TSE electrons, Cherenkov emission was described as a two-dimensional function of absorption and reduced scattering coefficients. Although biological tissue and silicone phantoms produced different absolute signals, their normalized optical-property trends were similar. Realistic TOPAS electron phase-space data were then used for TrueBeam 6 MeV electron and 6 MV photon beams, with mean absolute deviations of 7.2% and 10.9%, respectively. Photon and electron beams showed different optical-property dependences, potentially related to their initial depth and angular distributions, which require further investigation.

CONTACT

Timothy Zhu, PhD
Professor
Dept of Radiation Oncology
University of Pennsylvania
3400 Civic Center Blvd
Timothy.Zhu@pennmedicine.upenn.edu

INTRODUCTION

Cherenkov imaging provides real-time visualization of surface dose during radiotherapy, but the detected signal depends on tissue optical properties, beam type, incidence angle, and viewing geometry. Our previous CPU-based model characterized optical-property effects using a simplified TSET electron source. Here, we extend that work with a CUDA-accelerated Monte Carlo framework driven by TOPAS electron phase-space data. We validate the simulation code, reassess optical-property effects, and investigate the Cherenkov emission for clinically relevant photon and electron beams.

METHODS AND MATERIALS

An in-house CUDA-based Monte Carlo code was developed to model wavelength-dependent Cherenkov photon generation and transport from 400–900 nm in homogeneous turbid media (*g* = 0.9, *n* = 1.4). The simulation was validated using nine silicone phantoms with different concentrations of carbon absorber and TiO_2 scatterer. A simplified source consisting of normally incident electrons uniformly distributed from 0–1 cm beneath the surface was used, and simulated Cherenkov emission was compared with experimental measurements. The validated model was then used to systematically investigate optical-property dependence in biological tissue and silicone phantoms. Total Cherenkov emission was evaluated as a function of absorption, reduced scattering, effective attenuation, and diffuse reflectance, and the results were normalized to a reference phantom for relative comparison.

Further, realistic electron phase-space data were generated in TOPAS for TrueBeam 6 MeV electron and 6 MV photon beams at multiple depth. Cherenkov photons were sampled from the energy, direction, and depth of each scored electron to analyze depth- and angle-dependent production and compare simulated emission with measurements for both beam types.

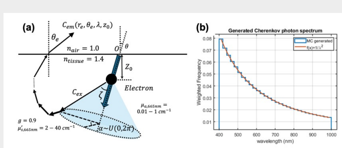

Figure. 1 (a) Setup geometry for Monte-Carlo simulation for a semi-infinite turbid medium. (b) Initial Cherenkov photon spectrum

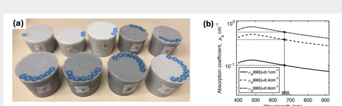

Figure 2. (a) Picture of 9 solid silicone gel phantoms made of carbon powder as absorber and TiO2 as scatterer. (b) Absorption coefficient spectra of carbon for μ_a= 0.1, 0.4, and 0.6 cm^{-1} at 665 nm.

RESULTS

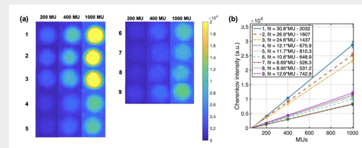

Figure 3. (a) Acquired Cherenkov images for 9 phantoms irradiated with HDTSE 6MeV electron beam at 200, 400 and 1000 MU at SSD 500 cm. (b) Cherenkov intensity versus MU for 9 phantoms (symbols) with different tissue optical properties (see Table 1). The lines are linear fits.

μ_a cm^{-1}	μ'_s cm^{-1}	Experiment	MC sim	Diff(%)
0.11	6.89	2.43	2.63	−7.6
0.11	10.88	2.30	2.30	0.0
0.11	20.35	2.01	2.10	−4.3
0.40	6.89	1.04	1.03	0.1
0.40	10.88	1.00	1.00	0.0
0.40	20.35	0.89	0.91	−1.8
0.61	6.89	0.72	0.74	−3.0
0.61	10.88	0.71	0.77	−7.1
0.30	20.35	1.09	1.10	−1.5

Table 1. Simulation vs Experiment for 9 optical phantoms. Simple electron source is used (1MeV pencil beam, uniformly distributed at 0-1 cm on the central axis, normal incident).

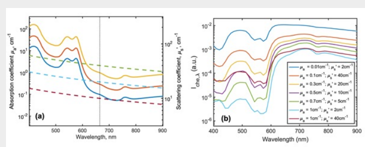

Figure 4. (a) Absorption coefficients and reduced scattering coefficients for the biological tissue. The absorption spectra (solid lines, μ_a = 0.1, 0.3 and 1.0 cm^{-1} at 665 nm) was calculated based on the extinction coefficient spectra of oxygenated and deoxygenated hemoglobin at 70% tissue oxygen saturation (StO2). The dashed lines are reduced scattering coefficients (μ_s'= 10, 20, 40 cm^{-1} at 665 nm), which are fitted by Mie scattering. (b) Simulated Cherenkov emission spectra for the biological tissue with 7 different tissue optical properties.

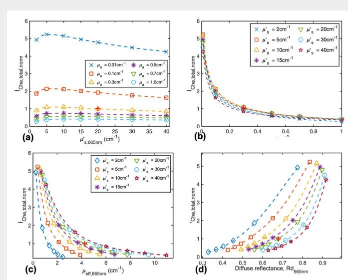

Figure. 5 Normalized Cherenkov emission intensity as a function of (a) reduced scattering coefficient, (b) attenuation coefficient (c) effective attenuation coefficient, (d) diffuse reflectance at 665 m.

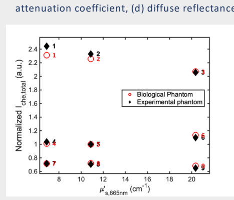

Figure. 6 Comparison of the total Cherenkov emission using the experimental phantom spectrum (figure2b, shown as black diamonds) and biological tissue spectrum (figure3, shown as red circles). The total Cherenkov emission are normalized at phantom 5 for all nine phantoms.

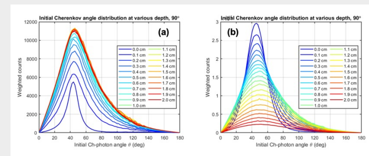

Figure. 7 Angular distribution of initial Cherenkov photons at multiple depths for (a) TrueBeam 6X photon and (b) TrueBeam 6MeV electron. Cherenkov photons generated from the electron phase space scored in TOPAS at 100cm SSD.

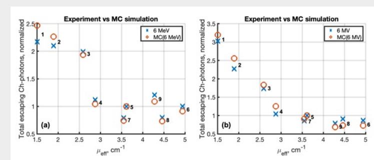

Figure. 8 Comparison of the experiment measurements (cross) and MC simulations (circle) under (a)TrueBeam 6MeV electrons and (b) TrueBeam 6MV photons, for nine phantoms with different optical properties. The values are normalized to phantom 5 to make direct comparison.

DISCUSSION

A GPU-accelerated Monte Carlo framework was developed to enable high-statistics simulations using realistic electron phase-space data, which were impractical with the previous CPU-based implementation. For TSE electron beams, surface Cherenkov emission can be described as a two-dimensional function of the absorption and reduced scattering coefficients. Although absolute emission differs between biological tissue and silicone phantoms, the normalized trends in Figure 6 are similar, suggesting that spectral shape has a smaller effect on relative optical-property dependence than on absolute emission. This also supports the use of silicone phantoms for evaluating relative optical-property effects, while highlighting the importance of spectral composition for absolute comparisons. Further, photon and electron beams showed different optical-property dependences, potentially due to differences in the initial depth and angular distributions of generated Cherenkov photons, which will be investigated in the future.

REFERENCES

1. Ong YH, Li AQ, Zhu TC. Monte Carlo investigation of the effect of skin tissue optical properties on detected Cherenkov emission. Proc SPIE Int Soc Opt Eng. 2019 Feb;10862:108621D.
2. Zhong W, Ong YH, Zhu T. Monte Carlo (MC) study of dose distribution and Cherenkov imaging in total skin electron therapy (TSET) with TOPAS. Proc SPIE Int Soc Opt Eng. 2021 Mar;11628:116280S

ACKNOWLEDGEMENT

This research is supported by National Institute of Health (NIH) grant R21 CA239127 and R01 CA274411.